

# Influence of water-cement ratio on micro-cracking of ordinary concrete

G. PROKOPSKI

*Civil Engineering Department, Technical University of Czestochowa, Armii Krajowej 27,42-200 Czestochowa, Poland*

The influence of the water/cement ratio on fracture toughness of ordinary concrete has been investigated. The stress intensity factor  $K_{IIc}$  and fracture energy  $J_{IIc}$  has been tested (Mode II, shearing). The concrete structure was examined by SEM and the influence of water/cement ratio on concrete cracking has been established.

## 1. Introduction

The majority of papers concerning the influence of the water/cement ratio (w/c-ratio) on concrete strength is limited mainly to determination of such parameters as minimum quantity of water which would be sufficient for complete cement saturation and the resulting greatest density of cement paste, mortar or concrete.

Recently, investigations of the influence of the w/c-ratio on fracture toughness of concrete has been undertaken. The results of these investigations, however, are rather contradictory.

According to Higgins and Bailey [1] an increase of w/c-ratio causes a decrease of fracture toughness and strength of the concrete, but Naus and Lott [2] have stated that this is valid only for cement pastes and mortars since in concretes the fracture toughness is independent of the w/c-ratio.

It has also been observed that at constant load the time to failure decreases with a rise in relative humidity for which the specimens reach a state of equilibrium, whereas the excessive quantity of water may produce easier growth of the primary fissure. It is also recorded that the fracture energy is smaller for wet specimens than for dry ones. In [3] it is shown that water absorption results in expansion of gel in the cement paste and thus decreases the value of fracture energy. On the other hand, Glücklich and Corin [4] have stated that a decrease of fracture energy is caused by water absorption and by saturation of settings inside gel. Therefore, the problem of the influence of water-quantity in concrete on the change of fracture energy and fracture toughness of concrete is neither solved nor clarified.

## 2. Experimental procedure

In this paper an attempt is made to establish the influence of water/cement ratio on the fracture energy and fracture toughness of ordinary concrete with regard to the mechanism of cracking. Ordinary concrete containing coarse aggregate 2-6.3 mm in size has been tested. Each group of specimens was prepared for

a w/c-ratio in the range 0.55-0.90, in increments of every 0.05.

The following investigations have been carried out:

- tests of the stress intensity factor  $K_{IIc}$  (mode II shearing);
- tests of the fracture energy  $J_{IIc}$ ;
- microscopic tests using a Cambridge Scientific S4-10 electron microscope.

The compressive strength of concretes was tested with the use of 3 concrete cubes (of side = 0.15 m) whereas the examination of fracture toughness was performed on 6 cubes (of side = 0.15 m) having two notches. Such a batch of specimens was made for each w/c-ratio tested.

All concrete mixes were made from the same components, using the same method of consolidation. The elements, by weight, were: gravel aggregate ( $1160 \text{ kg m}^{-3}$ ); quartz sand, 0-2 mm ( $760 \text{ kg m}^{-3}$ ); Portland cement, "35" ( $310 \text{ kg m}^{-3}$ ); and water  $w = c(0.55-0.90) \text{ l m}^{-3}$ .

The concrete mixes had the following consistences:

- at w/c = 0.55 and 0.60 → wet
- at w/c = 0.65 and 0.70 → plastic
- at w/c = 0.75 and 0.80 → half-liquid
- at w/c = 0.85 and 0.90 → liquid.

The samples were cured for seven days in a water bath and then stored in normal laboratory conditions for 21 days. After 28 day curing period they were subjected to fracture toughness tests.

The strength of concretes after pressure test is shown in Table I.

### 2.1. Fracture toughness test

The fracture toughness tests, performed according to mode II of cracking (shearing), are particularly important in determining the strength of cement pastes, mortars, concretes and other cement-base materials, since their shearing strength is relatively low. They were carried out, according to a concept presented in [5], using double-notch cubic samples as proposed by

TABLE I The strength of concretes after pressure test

w/c-ratio	0.55	0.60	0.65	0.70	0.75	0.80	0.85	0.90
Strength after pressure test	26.4	23.6	22.3	19.5	16.8	14.0	13.6	10.5
$\bar{R}$ [MPa] $\pm$ standard deviation	1.3	1.2	0.8	1.1	1.4	1.0	0.7	0.9

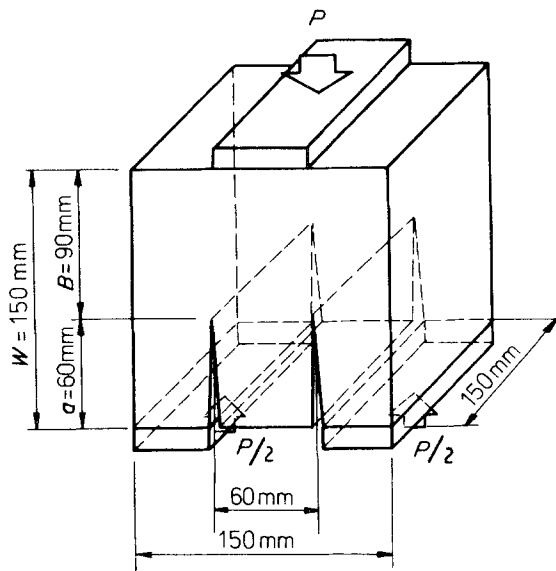


Figure 1 Test sample.

Watkins [6]. He showed (Fig. 1) that there is a wide range of independence of geometric size of sample,  $a/W$ , from compliance,  $Y(a/W)$ , to the tested stress intensity factor  $K_{IIc}$ .

By the finite element method Dixon and Strannigan [7] derived a formula in which the stress intensity factor  $K_{IIc}$  depends on a critical value of force  $P_Q$

$$K_{IIc} = \frac{5.11 P_Q}{2BW} (\pi a)^{1/2} \quad (1)$$

where  $P_Q$  is the force initiating cracking (growth), which is identified in graphs as a minor deflection or extremum of the curve;  $B$  is the thickness under crack;  $W$  is the height; and  $a$  is the length of the crack.

A Mode II fracture test was carried out on the stand presented in Fig. 2. The load was measured with a strain gauge against crack displacement and registered on an x-y plotter. The loading rate was  $\sim 200 \text{ N s}^{-1}$ .

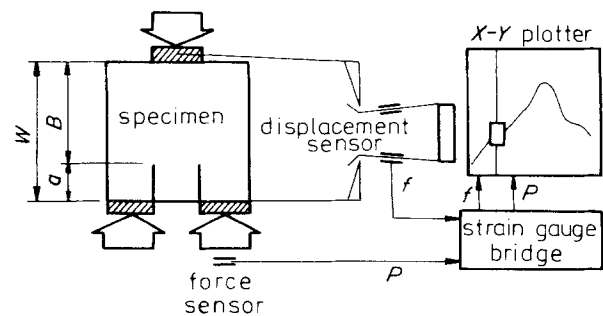


Figure 2 Scheme of test stand.

Table II contains values for the stress intensity factor,  $K_{IIc}$ , for each batch of specimens, characterized by an individual w/c-ratio.

The load-crack displacement curve was obtained for each specimen. Some specimen curves are shown in Fig. 3.

In Fig. 4 the stress intensity factor  $K_{IIc}$  is plotted against the w/c-ratio.

## 2.2. Determination of fracture energy

The diagrams of load against crack displacement obtained in the fracture toughness tests were used to determine the fracture energy according to a formula derived from [8]:

$$J_{IIc} = \frac{A}{2BW} \quad (2)$$

where  $A$  is the work done in destroying the sample (the field below the curves),  $B$  is the thickness,  $W$  the height, and  $a$  the length of the crack. Fracture energies, as obtained, are shown in Table III and Fig. 5.

The relationship of fracture energy  $J_{IIc}$  against the w/c-ratio indicates a strong monotonical decrease of fracture energy with increasing value of water/cement ratio.

TABLE II Stress intensity factor  $K_{IIc}$

w/c-ratio	0.55	0.60	0.65	0.70	0.75	0.80	0.85	0.90
$K_{IIc}$	1.887	1.800	1.91	2.182	1.831	1.631	1.505	1.44
( $\text{MN m}^{-3/2}$ )	4.438	2.239	1.937	2.247	1.887	2.177	1.865	2.16
	3.613	2.785	2.147	3.011	1.913	2.204	1.935	2.16
	3.24	2.963	3.419	3.176	2.165	2.403	2.012	2.238
	3.24	3.275	3.789	3.254	2.846	2.486	2.199	2.846
	3.06	3.375	3.948	3.254	3.093	2.846	3.131	2.093
	2.923	4.534	-	-	-	-	-	-
Mean value	3.20	2.996	2.858	2.854	2.286	2.282	2.108	2.156
Standard deviation	0.709	0.813	0.878	0.46	0.497	0.372	0.503	0.408

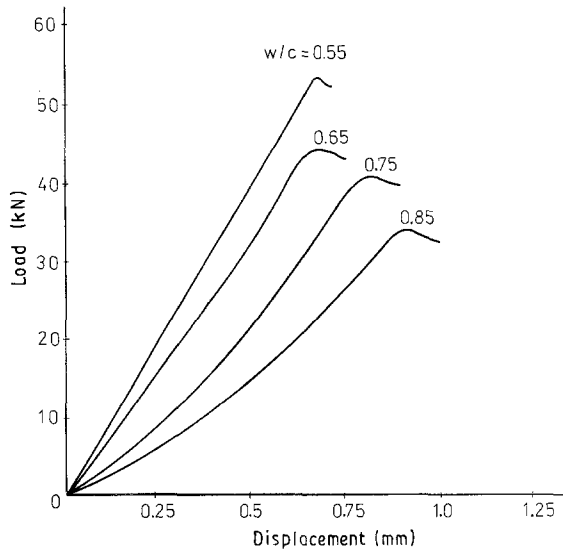


Figure 3 Load-displacement curves for various values of w/c-ratio.

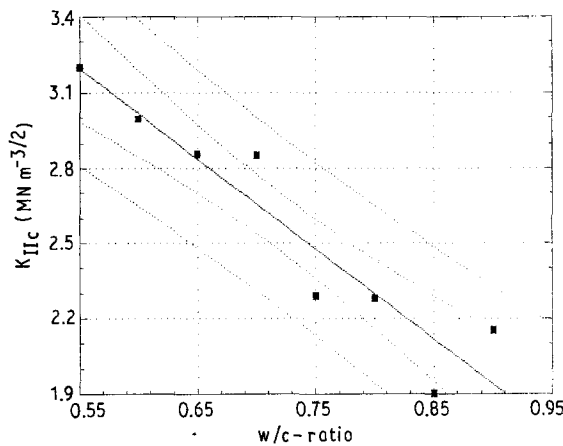


Figure 4 Relationship between water/cement ratio and stress intensity factor  $K_{IIc}$ .  $K_{IIc} = (5.168 \pm 0.739) \pm (3.587 \pm 1.006) w/c$ .  $R^2 = 0.8888$ ,  $\alpha = 0.0005$ .

### 2.3. Mechanism of microfracture

In order to estimate the mechanism of concrete microfracture depending on w/c-ratio, the SEM tests of selected concrete specimens was performed at magnifications  $\times 1000$  and  $\times 2000$ . Analysis of the micrographs showed that for lower values of the w/c-ratio (0.5–0.70) the predominant element of the concrete

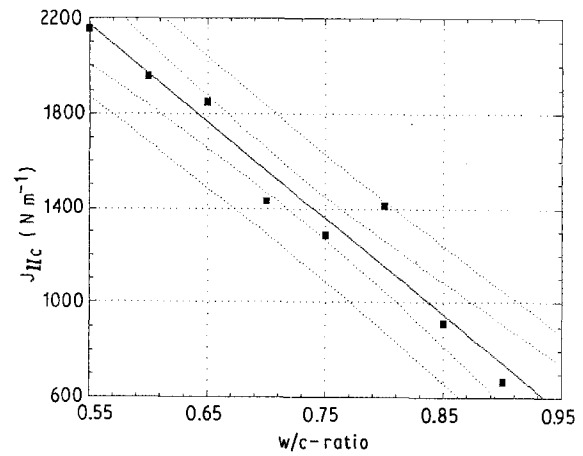


Figure 5 Relationship between water/cement ratio and fracture energy  $J_{IIc}$ .  $J_{IIc} = (4417 \pm 579) \pm (4080 \pm 789) w/c$ .  $R^2 = 0.9439$ ,  $\alpha = 0.0006$ .

microstructure are the grains of  $C_3S$  regularly distributed in cement gel (Fig. 6). In this case microcracks were propagating along the grain boundaries and they exhibited a complicated branched pattern. With an increase in the w/c-ratio in concrete the number of  $Ca(OH)_2$  crystals, located in layers, increased also.

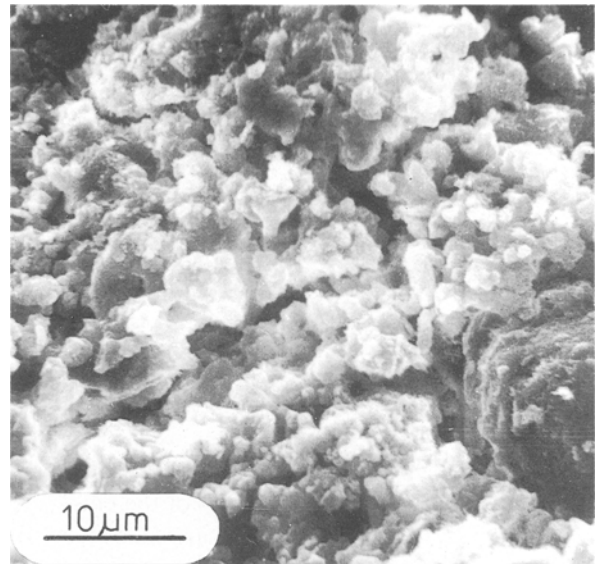


Figure 6 Intergranular fracture of sample with apparent  $C_3S$  grains. w/c = 0.70. Magnification  $\times 2000$ .

TABLE III Fracture energy  $J_{IIc}$

w/c-ratio	0.55	0.60	0.65	0.70	0.75	0.80	0.85	0.90
$J_{IIc}$ ( $N m^{-1}$ )	1053	849	2650	1210	1480	222	535	856
	2220	1400	1960	1290	1970	1220	1380	640
	2580	3100	1710	615	817	1000	785	549
	1770	1890	1080	859	957	1450	1210	384
	2735	1850	1950	2280	1340	1600	1080	797
	3040	2710	1750	2340	1140	1790	472	787
	1710	1920	—	—	—	—	—	—
Mean value	2158	1960	1850	1432	1284	1214	910	669
Standard deviation	640	700	463	660	378	510	288	164

These crystals, uniformly distributed in cement gel, are characterized by good adherence (Fig. 7). In this case the microfractures were propagating transgranularly through  $\text{Ca}(\text{OH})_2$  crystals and through the  $\text{Ca}(\text{OH})_2$  crystals/cement gel interface. Further increase of the w/c-ratio (Fig. 8, at w/c = 0.90) resulted in an increase of porosity and formation of calcium silicate in micropores. These calcium silicate crystals were in the fibrous form and produced a characteristic “fluffy” microstructure. The porosity of this structure was produced by capillary pores (Fig. 11) but in many regions the structural porosity was observed since the apparent volume of cement gel had not been filled by micelles (Fig. 8).

With the increase of water quantity in concrete the number of crystal types also increased ( $\text{Ca}(\text{OH})_2$ ,  $\text{C}_3\text{S}$  and  $\beta\text{-C}_2\text{S}$ ), as seen in Figs 10 and 11. Microcracks, in

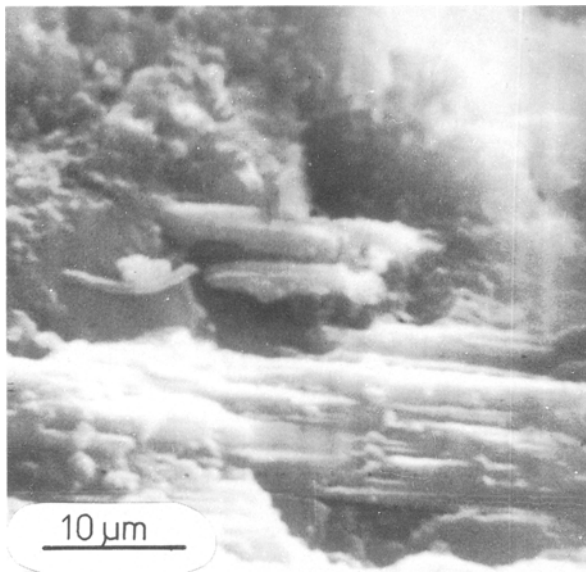


Figure 7 Cleavage fracture in  $\text{Ca}(\text{OH})_2$  crystals distributed in layers. w/c = 0.70. Magnification  $\times 2000$ .

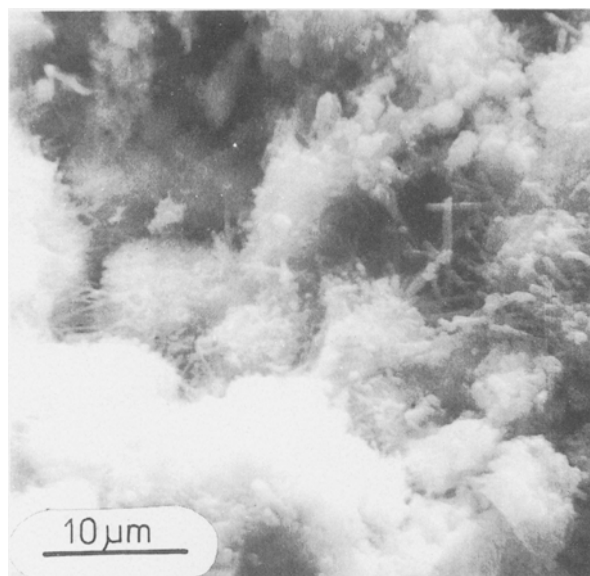


Figure 8 Calcium silicate hydrates in the form of thin fibrous crystals. w/c = 0.90. Magnification  $\times 2000$ .

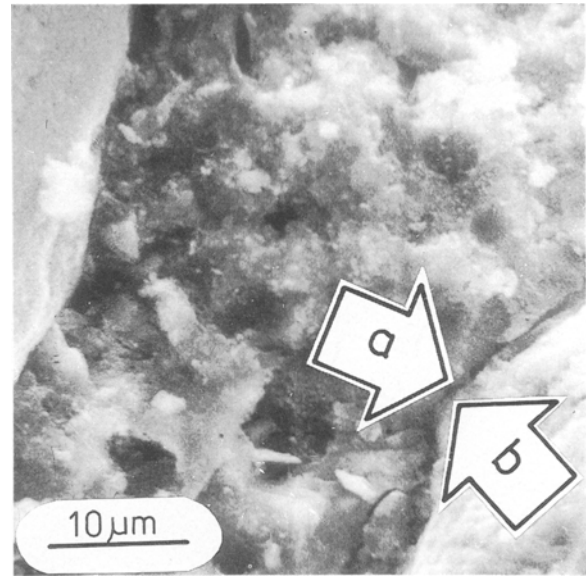


Figure 9 Microcrack on the gel/aggregate interface; a and b, respectively; capillary pores are shown. w/c = 0.60. Magnification  $\times 2000$ .

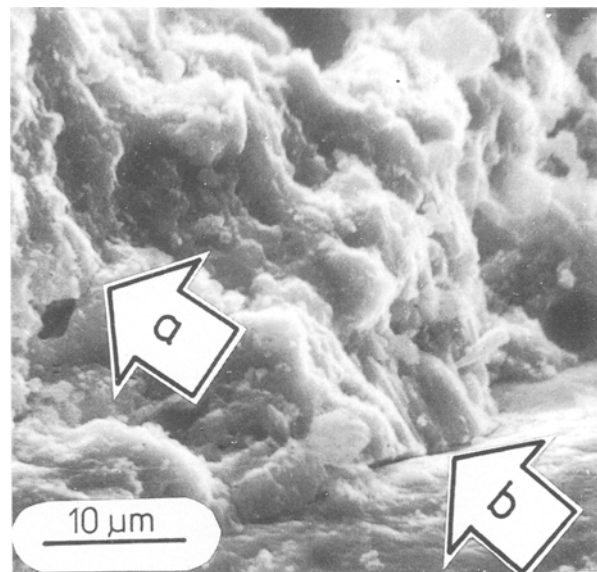


Figure 10 Cleavage cracks propagating through strongly developed  $\text{C}_2\text{S}$  and  $\text{C}_3\text{S}$  crystals (a) and aggregate/cement gel interface (b). w/c = 0.80. Magnification  $\times 2000$ .

this case, propagated along the crystal boundaries and through existing micropores. At greater w/c-ratios, increased quantities and dimensions of microfractures have been observed in the cement, paste/sand and gravel interface resulting in a loss of cohesion.

Therefore, the increased quantity of water in concrete has caused (i) an increment of quantity and dimensions of tougher crystal forms, and (ii) an increase of porosity (Figs 9 and 10). As a result a reduction of concrete fracture toughness was observed, as confirmed by the tests of the stress intensity factor  $K_{IIc}$  and fracture energy  $J_{IIc}$ .

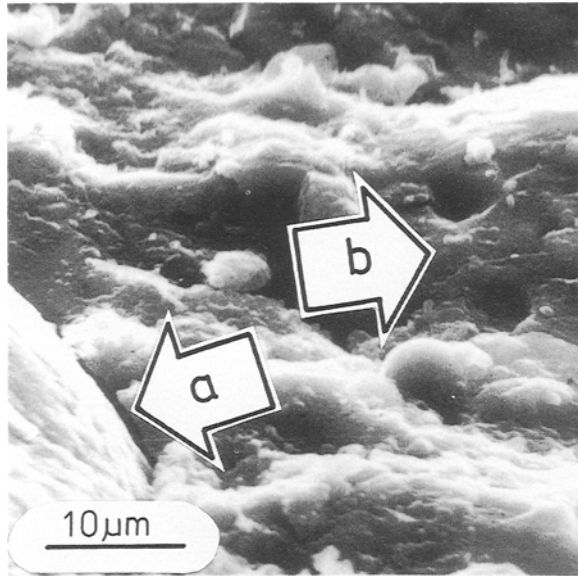


Figure 11 Microcracks propagating on cement paste/aggregate grain interface (a); capillary pores are seen (b).  $w/c = 0.70$ . Magnification  $\times 2000$ .

### 3. Conclusions

The proposed method of testing, based on mode II fracture, has shown the applicability of the stress intensity factor  $K_{IIc}$  and fracture energy  $J_{IIc}$  in estimating the concrete fracture toughness against water/cement ratio.

The tests of microstructure showed that the character of microcracks changes with the increase in the water/cement ratio. For lower  $w/c$ -ratios (0.55–0.70) the microcracks propagate intergranularly along the

grains of  $C_3S$  located in the cement gel. These microcracks had a strongly developed surface topography.

For higher  $w/c$ -ratios (0.75–0.90) an increase in porosity has been observed. The quantity and size of  $Ca(OH)_2$  crystals distributed in layers of cement gel increased also. The microcracks propagated transgranularly in  $Ca(OH)_2$  crystals and through the capillary and structural pores or along the fissures increasing in size, located on the grain boundary/cement paste interface.

The quantity of tougher crystalline forms observed on the micrographs increased with a rise in the  $w/c$ -ratio. However, it did not balance the loss of concrete fracture toughness caused by the rise of porosity. This resulted in the decrease of concrete fracture toughness with the increase of water/cement ratio.

### References

1. D. D. HIGGINS and J. E. BAILEY, *J. Mater. Sci.* **17** (1976) 1995–2003.
2. D. J. NAUS and J. L. LOTT, *J. American Concrete Institute* **6** (1969) 481–9.
3. D. J. COOK and M. N. HAQUE, *Cement and Concrete Research* **5** (1974) 735–44.
4. J. GLUCKLICH and U. CORIN, *J. American Ceramic Society* **1**(12) (1975) 517–21.
5. A. BOCHENEK and G. PROKOPSKI, *Int. J. Fracture* **41** (1989) 197–205.
6. J. WATKINS, *ibid.* **23** (1983) R135–R138.
7. J. R. DIXON and J. S. STRANNIGAN, *J. Strain Analysis* **7** (1972) 125–31.
8. “ $J_{IIc}$ , A Measure of Fracture Toughness”, ASTM E 813–81.

Received 9 May 1990

and accepted 31 January 1991